Potential synergic effect between MOR and BEA zeolites in NOx SCR with methane: A dual bed design approach

Acácio Nobre Mendes, Alexis Matynia, Alain Toullec, Sandra Capela,
M.Filipa Ribeiro, Carlos Henriques, Patrick da Costa

Potential synergic effect between MOR and BEA zeolitesin NO$_x$SCR with methane: a dual bed design approach

Acácio Nobre Mendes[1,2*], Alexis Matynia[2,3], Alain Toullec[2,3], Sandra Capela[4],M. Filipa Ribeiro[1], Carlos Henriques[1], Patrick Da Costa[2,3]

[1]Centro de Química Estrutural, Instituto Superior Técnico, Universidade de Lisboa. Av. Rovisco Pais, 1049-001 Lisboa, Portugal.

[2]Sorbonne Universités, UPMC,Univ. Paris 06, UMR 7190, Institut Jean le Rond d'Alembert, F-75005, Paris, France.

[3] CNRS, UMR 7190, Institut Jean le Rond d'Alembert, F-78210, Saint-Cyr l'Ecole, France.

[4]ENGIE, Research and Innovation Department, CRIGEN, 361 avenue du Président Wilson, 93211 Saint Denis La Plaine cedex France.

* Correspondingauthor: acacio.mendes@tecnico.ulisboa.pt

Graphical abstract

Highlights

- MOR and BEA zeolite catalysts containing Pd and Ce were prepared in a similar way.

- Characterisation evidenced different metal species in each catalyst.

- Catalyst exhibited different NO oxidation and NO$_x$ CH$_4$-SCR performances.

- Dual bed configuration revealed a potential synergic effect for NO$_x$ CH$_4$-SCR.

Abstract

The selective catalytic reduction of NO_x with methane (NO_x CH_4-SCR) under lean conditions was investigated with catalysts based on two different zeolite structures (MOR and BEA) containing Pd and Ce. The catalytic performance for NO oxidation to NO_2 reaction, considered an important first key step in the NO_x CH_4-SCR mechanism, was also assessed.

Pd(0.3)Ce(2)-HBEA was found to be very active for NO oxidation but exhibits poor activity for NO_x CH_4-SCR. Conversely, Pd(0.3)Ce(2)-HMOR presents modest activity for NO oxidation, compared to Pd(0.3)Ce(2)-HBEA, but exhibits mild activity for NO_x CH_4-SCR reaction. Characterisation by H_2-TPR, DRS UV-Vis, TEM/EDS and FTIR-CO allowed the identification of palladium stabilised as Pd^{2+} ions in exchange positions in both monometallic and bimetallic MOR based catalysts, whereas, in BEA catalysts, it is presented as PdO clusters. Cerium is stabilised in Pd(0.3)Ce(2)-HMOR as small CeO_2 particles, whereas, in Pd(0.3)Ce(2)-HBEA, it is present as large clusters. Catalysts were also tested in dual bed configuration, in which Pd(0.3)Ce(2)-HBEA was placed as first layer and Pd(0.3)Ce(2)-HMOR as second layer in the catalytic bed. The catalytic performance was significantly improved (higher NO_x conversion into N_2 and higher CH_4 selectivity to SCR reaction), when compared to the catalytic performance of each catalyst individually, suggesting the existence of a synergic effect. This synergy is explained by the complementary roles that each catalyst play in HC-SCR mechanism.

2

1. Introduction

The increasing concerns about air pollution control have recently resulted in the publication, by different countries, of legislation that establishesmore stringent maxima of allowed emission values for several pollutants (including nitrogen oxides, hydrocarbons and particulate matter), particularly in the road transportation sector (mobile sources)[1]. It is known that the importance of natural gas vehicles is increasing worldwide [2]. One possible after-treatment solution that simultaneously removes NO_x and HC from the exhaust gases of these vehicles, working in lean-burn conditions, is the NO_x selective catalytic reduction with hydrocarbons(HC-SCR) over zeolite-based catalysts containing metals[3-5].Despite several decades of studies, this technology still lacks some technological improvement in order to be successfully implemented as a commercial solution.

Pd-zeolites are known to be active for NO_xSCR using methane, under lean conditions, as a reductant[6-8]. The catalytic performance of these catalysts can be improved by considering bimetallic formulations, such as PdCo-zeolites[9, 10] and PdCe-zeolites[11, 12].Despite being active and selective catalysts, it has been reported in literature that PdCo-zeolites [13] suffer from deactivation over time, but the same seems not to happen with PdCe-zeolites, which activity has been reported to be constant over the time [14].Hence, the further understanding of the role of Ce in these catalysts might be important to move forward towards a commercial application of this type of after-treatment system.

Few works can be found in literature, describing the combination of different catalysts in dual catalysts systems as a possible solution for HC-SCR. For instance, Chen, *et al.* have reported the existence of synergies between different zeolites (namely, Fe-MFI and

Fe-FER) in the NO_x SCR with iso-butane [15]. Fe-FER presents lower activity NO_x SCR because the small pores of FER structure become blocked by nitrogen-containing compounds formed dueto the interaction between the hydrocarbons and NO_x. However, NO_2 is smaller enough to pass through the channels. On the other hand, Fe-MFI deactivates over time due to the formation of a deposit that blocks the sites responsible for the NO oxidation to NO_2, which is considered to be a first key step in the HC-SCR mechanism [16]. By mixing Fe-FER with Fe-MFI, the NO_2 formed in Fe-FER is able to interact with the active groups of the deposit on Fe-MFI and a resulting enhancement on catalytic performance is foreseen.

Holmgreen, *et al.*, havealso studied the use of dual catalysts system for HC-SCR in lean-burn conditions, namely using methane as reductant [17]. They observed an enhancing effect on NO_x SCR performance of Pd-supported sulphated zirconia (reduction catalyst), when mixedwith an oxidation catalyst, such as Co impregnated on zirconia (with low activity for NO_x SCR but high activity for NO oxidation to NO_2).

In this work, the catalytic performance of PdCe-zeolites (MOR and BEA) for NO_xSCR with methane is compared. The choice of these zeolites structures was based on the facts that (i) MOR is described in literature as azeolite structure that leads to active Pd and Pd-Ce catalysts for NO_x CH_4-SCR [12, 13, 18]; (ii) BEA zeolite has been used in a catalyst that exhibited enhanced catalytic performance for NO_x CH_4-SCR after being exposed to water [9], which is naturally present in realexhaust gases.Different characterisation techniques were used in order to identify the main differences in the metal species stabilised in the zeolite structures. A potential synergic effect on NO_x SCR with methane due to the mixture of the different zeolite-based catalysts containing identicalPd and Ce metal loadings is reported for the first time.

5

2. Experimental

2.1. Catalysts preparation

Catalysts were prepared from CBV21A zeolite (NH$_4$MOR), with Si/Al = 10 and CP814E zeolite (NH$_4$BEA), with Si/Al = 12.5, supplied by Zeolyst. In order to obtain Pd(0.3)-HMOR and Pd(0.3)-HBEA, 0.3 wt.% of palladium was introduced by ion-exchanging the starting zeolites with a solution with adequate concentration, prepared by dilution of a Pd(NH$_3$)$_4$(NO$_3$)$_2$aqueous solution (Aldrich, 99.99% purity, 10 wt.%), for 24h, at room temperature. Afterwards, exchanged samples were recovered by centrifugation and dried in an oven at 90ºC, overnight. Pd-zeolites were then calcined under air-flow, at 500 ºC, for 1 h (1ºC/min). Pd(0.3)Ce(2)-HMOR and Pd(0.3)Ce(2)-HBEA were obtained from Pd(0.3)-HMOR and Pd(0.3)-HBEA, respectively, by introducing 2 wt.% of cerium by incipient wetness impregnation technique, using a solution with adequate concentration, prepared with Ce(NO$_3$)$_3$.6H$_2$O salt (Fluka, 99% purity). Then, samples were dried in an oven at 90ºC, overnight, and finally calcined at 500 ºC, for 8 h (5 ºC/min).

2.2. Catalysts characterisation

Temperature programmed reduction under hydrogen (H$_2$-TPR) was performed by contacting a catalyst sample (*ca.* 100 mg) with a mixture of H$_2$ (5 vol.% in Ar, 30 mL/min) and heating it until 900ºC using a ramp of 7.5 ºC/min. Hydrogen consumption was measured with a thermal conductivity detector. Water was trapped in a dry ice-cooled trap.

Diffuse reflectance spectra in the UV-Vis range (DRSUV-Vis) were collected on a *Varian Cary 5000 UV-Vis-NIR* spectrophotometer equipped with a *Praying Mantis*accessory. Spectra were collected at room temperature, using calcined samples (range 200-800 nm, scan rate - 600 nm/min, data interval - 1 nm, SBW - 4 nm). Reflectance spectra were converted into the Schuster-Kubelka-Munk (SKM) function, F(R), calculated at each wavelength using the expression:

$$F(R) = \frac{(1-R)^2}{2R} \tag{1}$$

R is the ratio of the intensity of the light reflected by the sample to the one reflected by a standard. In order to minimise the effect of zeolite framework absorption, the standard considered was a parent HMOR and HBEA zeolite sample, obtained from NH_4MOR and NH_4BEA samples throughout the same calcination procedure described before, after cerium introduction in bimetallic samples.

Transmission electron microscopy (TEM) was performed on a *JEOL JEM 2010*microscope (LaB6 cannon) operating at 200 kV. Prior to TEM, samples were crushed and then dispersed with ethanol on a carbon-coated copper TEMgrid. Energy-dispersive X-ray spectroscopy (EDS) was also performed (probe PGT-Bruker).

CO adsorption followed by Fourier transform infraredspectroscopy was also performed in order to obtain further information regarding the physicochemical properties of the catalysts surface. Spectra were collected with a Nicolet 6700 FTIR spectrometer (400-4000 cm^{-1}, 128 scans, 4 cm^{-1} resolution). Self-supporting wafers of catalyst (*ca.* 10 mg/cm^2) were pre-treated by heating to 400 ºC at 3 ºC/min, then holding for 30 min, inside a vacuum cell (P < 10^{-4} Pa, equipped with CaF_2 windows) attached to the vacuum line. After pre-treatment, wafers were reduced at 400 ºC, for 1 h, under 100 torr of H_2. After reduction, the cell was evacuated for 10 min to P <10^{-5}torr. The wafers were then

cooled down to room temperature and a spectrum was collected prior to CO adsorption. Next, 5 torr of CO was introduced into the cell anda spectrum was obtained.The CO gas phase spectrum was collected. All spectra presented were obtained after subtracting CO gas phase and the activated sample (after reduction) contributions, and they were normalised at the same weight/surface wafer ratio.

2.3. Catalytic tests

Catalytic tests were performed in a tubular *pyrex* reactor using 190 mg of catalyst (dry basis) corresponding to a GHSV of 40000 h^{-1}. For the dual bed test, 95 mg of Pd(0.3)Ce(2)-HMOR were first loaded to the reactor, and then 95 mg of Pd(0.3)Ce(2)-HBEA were carefully loaded, in order to obtain two separate layers, so that the inlet gas mixture would contact BEA catalyst first. Before the reaction, a pre-treatment was performed consisting in heating the catalyst under argon flow (15 L/h), from room temperature to 500 ℃ (5 ℃/min) and keeping this temperature for 1 h, in order to clean the catalysts' surface. Then, the reactor was cooled to 300 ℃ still under argon flow. Meanwhile, the reaction mixture was stabilised in a reactor by-pass, using two four-way valves. Once stable, the reaction mixture was fed to the reactor. When the steady state was reached, the temperature was raised 50 ℃. This procedure was repeated until 500 ℃.

NO$_x$SCR tests were performed using a mixture of 1000 ppm NO, 1000 ppm CH$_4$, 7 vol.% O$_2$and 2 vol.% H$_2$O in flowing argon (total flow rate of 250 mL/min, GHSV = 40000 h^{-1}). NO oxidation to NO$_2$ tests were performed using a mixture of 1000 ppm NO and 7 vol.% O$_2$ in flowing argon (total flow rate of 250 mL/min, GHSV = 40000 h^{-1}).

The reactor's outflow was continuously analysed. NO and NO_2 concentrations were detected by a *Thermo 42C* chemiluminescence analyser. CO, CO_2 and N_2O concentrations were detected by an *ABB EL 3020* infrared analyser. A *Pfeiffer Vacuum GSD 301* mass spectrometer was also used to follow the reaction, namely the constant amount of water introduced in the inlet stream (m/z = 17 and 18).

For each temperature T, NO_x conversion into N_2 was obtained using equation (2), CH_4 conversion into CO_2 was obtained using equation (3) and selectivity of methane to SCR reaction was obtained using equation (4).

$$x_{NO_x\ to\ N_2,T}(\%) = \left(1 - \frac{n_{NO,T} + n_{NO_2,T} + 2\,n_{N_2O,T}}{n_{NO,0} + n_{NO_2,0}}\right) \times 100\% \tag{2}$$

$$x_{CH_4\ into\ CO_2,T}(\%) = \frac{n_{CO_2,T}}{n_{CH_4,0}} \times 100\% \tag{3}$$

$$S_{CH_4\ to\ SCR,T}(\%) = \frac{n_{CH_4\ for\ SCR,T}}{n_{CH_4\ converted,T}} = \frac{n_{NO,0} + n_{NO_2,0} - (n_{NO,T} + n_{NO_2,T} + 2\,n_{N_2O,T})}{n_{CH_4,0} - (n_{CO_2,T} + n_{CO,T})} \times 100\% \tag{4}$$

0 represents the initial condition (by-pass mixture) before starting the reaction.

3. Results and Discussion

3.1. Temperature programmed reduction under hydrogen (H$_2$-TPR)

Figure 1 shows the H$_2$-TPR profiles of the studied catalysts. The H$_2$-TPR profiles of both HMOR and HBEA catalysts, obtained by applying the same calcination procedure as the one described in the catalyst preparation section for bimetallic catalysts (after cerium introduction) did not exhibit any reduction process. For bothPd(0.3)-HMOR and Pd(0.3)Ce(2)-HMOR, it is possible to observe the existence of a reduction peak between 80-200 ºC, which is assigned to the reduction of Pd^{2+} in exchange positions to Pd^0[19-21].The integration of this peak results in a H$_2$/Pd ratio of*ca.* 1.1 for Pd(0.3)-HMOR, which is consistent with the stabilisation of all the palladium as Pd^{2+} in exchange position in literature[21]. For Pd(0.3)Ce(2)-HMOR, the integration of this peak results in a H$_2$/Pd ratio of *ca.* 1.8, which is significantly higher than the unity. In fact, the reduction of surface Ce^{4+} species to Ce^{3+}is known to take place in this range of temperatures [22], which explains this result.

For Pd(0.3)-HBEA, no reduction peak is observed in the entire range of temperatures. It has been reported in literature that palladium is stabilised in BEA zeolite as PdO, which reduction is likely to occur between -20 to 25 ºC [23], explaining the absence of reduction peaks in the H$_2$-TPR profile of Pd(0.3)-HBEA. However, when cerium is added to Pd(0.3)-HBEA, two reduction peaks are visible between 60-180 ºC (see H$_2$-TPR profile of Pd(0.3)Ce(2)-HBEA). The integration of first reduction peak, 60-120ºC, results in a H$_2$/Pd ratio of 0.4. One can speculate that the presence of Ce may promote the stabilisation of part of the palladium as Pd^{2+} ions in exchange position or, eventually, contributes for a more difficult reduction (*i. e.*at higher temperature) of part of the PdO. The second reduction peak, 120-180 ºC, is ascribed to the reduction of

surface Ce^{4+} species [22], similar to what happens for Pd(0.3)Ce(2)-HMOR (in order to provide a term of comparison between both bimetallic catalysts, the H_2/Pd ratio corresponding to the reduction peak of Ce^{4+} species in Pd(0.3)Ce(2)-HBEA is 0.17, significantly lower than in Pd(0.3)Ce(2)-HMOR = 1.8-1.1 = 0.9)

Finally, for both bimetallic catalysts, a broad reduction peak can be observed between 300-550 ºC, which can be attributed to CeO_2 species. The reduction of the most easily reducible surface capping oxygen of CeO_2 usually occurs at slightly higher temperatures (*ca.*500 ºC)[22]. However, due to interaction with other metal species, namely palladium, it has been reported a shift to lower temperatures[22, 24], which can explain the fact that this reduction process begins at 300 ºC. The integration of these peaks leads to a H_2/Pd ratio of 0.13 for Pd(0.3)Ce(2)-HMOR and 0.31 for Pd(0.3)Ce(2)-HBEA.

3.2. Diffuse reflectance UV-Visspectroscopy (DRSUV-Vis)

Figure2A and B illustrate the DRSUV-Vis spectra for both MOR and BEA catalyst series, respectively.For Pd(0.3)-HMOR, a single band is observed at approximately 400 nm, which is attributed to d-d transitions of Pd^{2+} ions [25]. This band appears slightly blue-shifted (385 nm) in Pd(0.3)Ce(2)-HMOR spectrum, which might be an effect of the presence of cerium. For the bimetallic MOR based catalyst, two additional bands can be clearly identified. The band at 260 nm is ascribed to the transition 4f-5d of Ce^{3+} species[26] and the band at 290 nm is characteristic of the charge transfer from O^{2-} to Ce^{4+} in CeO_2 clusters [26].

Pd(0.3)-HBEA exhibits a broad band at 335 nm, which is ascribed to charge transfer Pd→O[27]. For Pd(0.3)Ce(2)-HBEA, two additional bands at 260 and 290 nm appear overlapped with the previous mentioned band. These two bands are the same

onesobserved for Pd(0.3)Ce(2)-HMOR and can be ascribed to Ce^{3+} and Ce^{4+} species, respectively.

3.3. Transmission electron microscopy (TEM)

TEM images (Figure 3) allow to evidence significant differences in the Ce and Pd species that are stabilised in the studied zeolites (MOR and BEA).

No metal particles were observed in all TEM images collectedforPd(0.3)-HMOR sample (Figure 3A). Moreover, the several energy-dispersive X-ray spectroscopy (EDS) analyses performed did not detect the presence of palladium. However, H_2-TPR and DRS UV-Vis confirmed the existence of Pd species, which supports the idea that palladium is well dispersed in the catalyst as Pd^{2+} in exchange positions, which cannot be detected by TEM.

Small metal particles ($\bar{d}_p$ = 5 nm) can be observed in the external surface of the zeolite particles of Pd(0.3)Ce(2)-HMOR (Figure 3B). EDS analyses identified cerium as the element present in these particles. Moreover, high resolution TEM (HRTEM) allowed the quantification of the distance between lattice planes in 3.1 and 2.7 Å,typical from CeO_2 (ICDD 00-034-0394).The fact that palladium was not observed in TEM images, or detected by EDS, suggests that even after the addition of cerium to Pd(0.3)-HMOR, palladium remains stabilised as dispersed Pd^{2+} ions in exchange position.

Contrarily to Pd(0.3)-HMOR, TEM images of Pd(0.3)-HBEA reveal the existence of metal clusters in the external surface of the BEA zeolite particles (Figure 3C). EDS analyses confirmed that these are, indeed, palladium clusters and HRTEMallowed the quantification of the distance between lattice planes in 2.6 Å, typical from PdO (ICDD

12

00-041-1107).PdOclusters were also identified in Pd(0.3)Ce(2)-HBEA (Figure 3D). Moreover, CeO$_2$clusters were also identified in this catalyst. It is worthy to highlight that these cerium clusters are significantly larger than the CeO$_2$ particles detected in Pd(0.3)Ce(2)-HMOR.

Further results of the catalysts obtained by TEM can be found in the supporting data.

3.4. CO adsorption followed by FTIR spectroscopy

Figure 4 shows the FTIR spectra of the catalysts studied in this work, following adsorption of CO. For Pd(0.3)-HMOR, an intense band is observed at 2220 cm^{-1}. According to Hadjiivanov and Vayssilov[28], IR bands in 2215-2110 cm^{-1}spectral range have been attributed to linear Pd^{n+}-CO complexes.Although the 2220 cm^{-1} band appears slightly blue-shifted from the Pd^{n+}-CO spectral range, one could be led to ascribe this band to such species. However, as all catalyst were reduced prior to CO adsorption, this band is assigned to Al^{3+}-CO complexes [28-30], which was also confirmed by the CO adsorption experiments on Pd free HMOR.The formation of such complexes is likely to occurin the presence of CO interacting with theextra-aluminium species responsible for Lewis acidity, even at room temperature[18, 21]. A second band observed at 2198 cm^{-1}can be also ascribed to Lewis acid sites (LAS), which is in agreement with the results obtained by Reifsnyder, *et al.*[21].A low intensity band at 2169 cm^{-1} can be ascribed to Brønsted acid sites (BAS)[18, 21], or to residual Pd cationic species, for instance Pd^{2+}[28]. A weak band 2137 cm^{-1}also appears in the spectral range of Pd^{n+} carbonyls. It can beassignedPd$^+$-CO orPd$^{\delta+}$-CO complexes [21],which indicate the presence of cationic Pd species or small positively charged Pd clusters in the vicinity of BAS even after the sample reduction at 400 ºC. Bands below 2100 cm^{-1} are characteristic of CO

13

interactions with metallic palladium species[28]. The band at 2099 cm^{-1} is attributed to linear Pd^0-CO complexes, whereas the bands at 1962 and 1898 cm^{-1} are ascribed to bridging CO on Pd^0 clusters (two-fold and three-fold coordination, respectively[31]).

For Pd(0.3)Ce(2)-HMOR, similar bands are observed in the spectrum. However, two new and intense bands appear at 2188 cm^{-1} and 2355 cm^{-1}.According to Hadjiivanov and Vayssilov, carbonyls formed with cerium ions have characteristic bands in the spectral region of 2190-2110 cm^{-1}[28]. One can ascribed the band at 2188 $cm^{-1}$to Ce^{n+}-CO complexes (Ce^{3+} or Ce^{4+}). Indeed, in the DRS UV-vis spectrum of Pd(0.3)Ce(2)-HMOR (Figure 2a), absorption bandscharacteristic of both species have been observed. The band 2355 cm^{-1} is attributed to linear CO_2[32], which is likely to result from the oxidation of CO to CO_2 on the cerium sites. A significantly less intense band, at 2290 cm^{-1}, is also observed in the spectrum and is likewise attributed to CO_2 complexes. Though the bands at 2141 and 2123 $cm^{-1}$are within the spectral range of Ce^{n+}-CO complexes, these bands might be also due toPd^{n+}-CO complexes. In fact, it is likely that the presence of CeO_2 (also detected by H_2-TPR and TEM – Figure 1 and 3B, respectively) attenuates the reduction of Pd species or promotes its re-oxidation. At the same time, some of the palladium is presented in metallic form, which is evidenced by the characteristic bands at 2101, 1959 and 1894 cm^{-1}.

For the reduced Pd(0.3)-HBEA catalyst, two bands at 2226 and 2188 cm^{-1}, can be observed in the CO spectrum, which are attributed to LAS of BEA zeolite [33, 34], similarly to what was observed for Pd(0.3)-HMOR. In addition, for Pd(0.3)-HBEA, the bands attributed toPd^{n+}-CO complexes are not observed. For metallic Pd species, typical bands of linear Pd^0-CO complexes (around 2100 cm^{-1}) are not visible,and only a band characteristic of bridging CO in Pd clusters is observed at 1894 cm^{-1}. This result supports the idea that, conversely to Pd(0.3)-HMOR, Pd is lesswell dispersed in the

BEA structure, resulting in the formation of larger Pd^0 species. This in agreement with the TEM/EDSdata, which confirms the presence of PdO clusters (before reduction). In Pd(0.3)-HBEA spectrum, a low intensity band at 2363 cm^{-1} is observed, which could be ascribed to CO_2 complexes. One can speculate that part of Pd^0 clusters might have been re-oxidised leading to the formation PdO, which would be responsible for CO oxidation to CO_2.

In the spectrum of Pd(0.3)Ce(2)-HBEA the bands at 2226 and 2188 $cm^{-1}$are more intense than those previously observed in Pd(0.3)-HBEA. This could be due to a higher number of LAS in this catalyst after the introduction of cerium. Alternatively, the increase in intensity of the 2188 cm^{-1}band could be related to the presence of Ce^{n+} or Pd^{n+} species. In fact, an additional band is observed at 2127 cm^{-1} which could be attributed to Pd^+-CO complexes. Moreover, unlike for Pd(0.3)-HBEA, bands at 2107 and 1972 cm^{-1} are observed in Pd(0.3)Ce(2)-HBEA, which suggests the existence of an higher relative amount of metallic palladium in smaller clusters allowing linear and two-fold bridging coordination. These results indicate that the presence of cerium oxide may promote the re-dispersion of Pd in BEA structure. Finally, the band at 2358 cm^{-1} is assigned to linear CO_2, which is in agreement with the observation for Pd(0.3)Ce(2)-HMOR.

3.5. Catalytic tests

3.5.1. NO oxidation to NO_2

According to literature, NO oxidation to NO_2 is a first key step in the NO_xSCR mechanism when using hydrocarbons as reductant (HC-SCR)[16].Hence, the catalytic performance for this reaction was assessed (Figure 5). Pd(0.3)-HMOR shows a poor

activity for NO oxidation and even Pd(0.3)Ce(2)-HMORexhibits a modest activity for NO oxidation. However, Pd(0.3)-HBEA shows to be considerably active for this reaction. Moreover, Pd(0.3)Ce(2)-HBEA shows to be very effective in oxidising NO to NO_2, with the conversion values very close to the thermodynamic equilibrium in practically the entire range of tested temperatures.

Cerium is well known to catalyse NO oxidation [11].In fact, FTIR-CO spectra of both Pd(0.3)Ce(2)-HMOR and Pd(0.3)Ce(2)-HBEA exhibit very intense bands attributed to the formation of CO_2 complexes that resulted from CO oxidation (Figure 4), oppositely to what was observed for monometallic catalysts. When looking to each catalyst series separately (MOR and BEA), the presence of cerium in the bimetallic formulation explains the higher NO oxidation values of these catalysts when compared to their equivalent monometallic catalysts.

It is interesting to note thatPd(0.3)-HMOR and Pd(0.3)-HBEA exhibit very different catalytic performances for this reaction. The poor catalytic activity of Pd(0.3)-HMOR can be attributed to the fact that practically all palladium is stabilised as Pd^{2+} ions instead of PdO, which is a species known to promote oxidation reactions (*e.g.*CH_4 oxidation[35]).

3.5.2. NO_xSCR with CH_4

The results for NO_xSCR tests are illustrated in Figure 6 (N_2O and CO formation are negligible).It is possible to observed that MOR based catalysts are more active for NO_x SCR reaction than BEA based catalysts. This result was quite unexpected considering the very high activity for NO oxidation, observed for BEA based catalysts. It must be highlighted that even non-selective total oxidation of methane was quite poor.Active Pd-zeolites are known to lose activity when, under certain conditions, Pd tends to

16

agglomerate into large PdO clusters, *i. e.*, due to loss of Pd dispersion[8, 12]. The fact that Pd is stabilised as Pd^{2+} in exchange positions in both Pd(0.3)-HMORand Pd(0.3)Ce(2)-HMOR and as PdOclusters in Pd(0.3)-HBEA and Pd(0.3)Ce(2)-HBEA,might explain the differences on the catalytic behaviour. Also, the fact thatthis latter catalyst presents a notable performance for NO oxidation but very poor activity for NO_xSCR, indicates that the presence of Pd^{2+}ions in exchange positions is crucial for this reaction, which has already been reported in literature [8].

It is known that the addition of Ce to Pd-zeolite catalysts enhances the catalytic performance[12]. In fact, the NO_x conversion values are higher for Pd(0.3)Ce(2)-HMOR when compared to Pd(0.3)-HMOR. This enhancing effect is attributed to different roles of Ce: (i) the promotion of NO oxidation to NO_2[11]; (ii) the stabilisation of Pd^{2+} ions in the most active exchange positions [11, 12]; (iii) inhibition of the formation of PdO particles [12]. These latter two effects can be justified by an interaction between Pd and Ce species. H_2-TPR profiles evidence that this interaction in Pd(0.3)Ce(2)-HBEA is more extensive than in Pd(0.3)Ce(2)-HMOR (the H_2/Ce ratio obtained by the quantification of the reduction peak between 300-550ºC is higher for Pd(0.3)Ce(2)-HBEA). However, by crossing this information with the catalytic test results, it seems that the pertinent interaction between Ce and Pd from the NO_x SCR point of viewneeds, necessarily,to involve Pd^{2+} ions (instead of PdO).

In general, one can say that the NO_x conversion values obtained for the catalytic tests are not particularly high, especially when comparing with similar systems described in literature (*i.e.*PdCe-based systems, namely considering MOR as support). However, it should be highlighted that the catalytic test conditions considered in this this work are significantly less favourable when compared with other studies (Table 1).

For instance, Pieterse, *et al.*[14] reported a NO_x conversion of *ca.* 60%, at 375 ºC, with Ce-Pd-MOR (0.4 wt.% Pd and 2-4 wt.% Ce). However, the catalytic tests were performed with a feed of 500 ppm NO, 2500 ppm CH_4, 5 wt.% O_2 and 5 vol.% H_2O,*i.e.*, using $[CH_4]/[NO]$ ratio in the inlet feed of 5. The authors obtained even higher NO_xconversions, *ca.* 80% and 100% using inlet feeds with $[CH_4]/[NO]$ ratio of 7 and 19, respectively. In this work, the $[CH_4]/[NO]$ ratio considered was 1, which represents significantly less reductant. Moreover, the GHSV value considered in the previous mention study was 17000 h^{-1}, which is less than half of the value considered in this study (40000 h^{-1}).

Also, Costilla, *et al.*[12] reported a NO_x conversion of *ca.* 65%, at 500 ºC, with Ce-Pd/H-MOR (0.2 wt.% Pd and 2 wt.% Ce). In this case, the authors considered a feed of 1010 ppm NO, 3300 ppm CH_4, 4.1 vol.% and 5 vol.%H_2O., consisting in a $[CH_4]/[NO]$ > 3, and a GHSV = 33000 h^{-1}. Once again, this consists in a favourable situation compared to one considered in this work.

Different studies involving other catalytic systems have been conducted considering similar feed mixtures. For instance, Gutierrez and Lombardo [36] reported a NO_x conversion of *ca.* 40%, at 500 ºC, with CoLa-HMOR catalysts (1.7 wt.% Co and 1.2 wt.% La), considering a feed of 1000 ppm NO, 1000 ppm CH_4, 2 vol%. O_2 and 10 vol.% H_2O. Notwithstanding, the GHSV considered was 7500 h^{-1}, *i.e.*, five times lower that the one consider in the present work.Gutierrez, *et al.*[37] conducted a catalytic test with PtCo-MOR (0.39 wt.% Pt and 2.87 wt.% Co) with a feed containing 1000 ppm NO, 1000 ppm CH_4, 2 vol%. O_2 and 2 vol.% H_2O, where they observed a NO_x conversion of 36%, at 500 ºC, considering a GHSV = 30000 h^{-1}. The conversion value is slightly higher the ones obtained in this work, but the GHSV is also lower.

18

Due to the complementary catalytic performances of both bimetallic catalysts (Pd(0.3)Ce(2)-HMOR shows poor NO oxidation activity and is mildly active for NO_xSCR, whereas Pd(0.3)Ce(2)-HBEA exhibits high NO oxidation activity but is inactive for NO_xSCR), a test considering a dual bed of both catalysts was performed to assess theeventual existence of synergies between them. If no synergy took place, one would expect that the conversion values forsuch test would be lowerthan the ones obtained for Pd(0.3)Ce(2)-HMOR due to a dilution effect of Pd(0.3)Ce(2)-HMOR by the inactive Pd(0.3)Ce(2)-HBEA on the catalytic bed (only 95 mg against 190 mg). However, results show that the NO_x conversion achieved by dual bed is higher than Pd(0.3)Ce(2)-HMOR and, also, CH_4 conversion to CO_2 is lower.

Infact, when analysing the values of selectivity of CH_4 to SCR reaction for both dual bed and Pd(0.3)Ce(2)-HMOR catalysts (Figure 7), it is possible to observe that these values are higher in the case of dual bed catalyst. This means that, with this configuration, more CH_4 is being effectively used as a reductant, instead of being directly oxidised to CO_2 (combustion). This fact evidences a clear improvement in the catalytic performance.

According to the NO_x HC-SCR mechanism proposed Djéga-Mariadassou and co-workers, the NO_x SCR reaction passes by three different reactions, each one corresponding to a cycle or function [16, 38], which are illustrated in Figure 8. The first cycle (F1) consist in the oxidation of NO to NO_2. The NO_2 will then partially oxidise the hydrocarbons to $C_xH_yO_z$ intermediary species (second cycle – F2) which are, indeed, the actual reductant responsible for regenerating the active sites involved in the direct decomposition of NO to N_2 (third cycle – F3).

The interpretation of the results suggests that a low performance of Pd(0.3)Ce(2)-HMOR for NO oxidation is limiting, up to some extent, its NO_x SCR performance, in particular, the catalytic function F1 of the 3-function HC-SCR mechanism proposed in literature[16, 38].

In the dual bed configuration, where the inlet gas mixture first contacts with Pd(0.3)Ce(2)-HBEA, a high amount of NO_2 is expected to be formed (see Figure 4). Then, when it reaches Pd(0.3)Ce(2)-HMOR, it is likely that products resulting from the interaction of NO_2 and CH_4 can be produced (R-NO_x species) and, subsequently, decomposed in partial oxidised hydrocarbons ($C_xH_yO_z$) and NO (F2 of the mechanism). These $C_xH_yO_z$ species have been identified as intermediate products, resulting from the NO_2-CH_4 interaction [38] and are believed to be required to regenerate the catalytic sites responsible for the direct decomposition of NO into N_2 (function F3 of the mechanism).

4. Conclusions

The use of different zeolites (BEA and MOR) in the preparation of bimetallic catalysts, containing similar amounts of metal, by addition of cerium to Pd-based catalyst resulted in two catalysts with completely different catalytic performances.Pd(0.3)Ce(2)-HBEA has shown to be very effective in oxidising NO to NO_2 and significantly better than Pd(0.3)Ce(2)-HMOR. This reaction is considered to be a first key step on the NO_x SCR mechanism using hydrocarbons (HC-SCR). However,Pd(0.3)Ce(2)-HMOR revealed to be active for NO_xSCR with CH_4, whereas Pd(0.3)Ce(2)-HBEA exhibited a poor catalytic performance in the conditions considered in this study.

A combination of different characterisation techniques allowed to identify important differences in the metal species present in both MOR and BEA catalysts.

In Pd(0.3)-HMOR, palladium is stabilised as Pd^{2+} in exchange positions, whereas it is stabilised as PdO particles in Pd(0.3)-HBEA. In Pd(0.3)Ce(2)-HMOR, cerium is presented as small CeO_2 particles, whereas in Pd(0.3)Ce(2)-HBEA, cerium is stabilised in large clusters of CeO_2 distributed in the external surface of the zeolite, which are likely to be responsible for the NO oxidation performance. The palladium species are kept as Pd^{2+} in exchange positions in Pd(0.3)Ce(2)-HMOR and PdOclusters in Pd(0.3)Ce(2)-HBEA. The lack of Pd^{2+} explains the low activity of BEA catalysts for NO_xSCR reaction.

A synergic effect was observed in the NO_xSCR performance when both bimetallic catalysts were tested in dual bed configuration.This synergy can be explained by the complementary catalytic behaviour of both catalysts in performing the different function of HC-SCR mechanism.

Acknowledgements

References

[1] European Union, website, Summaries of EU Legislation - Reduction of pollutant emissions from light vehicles, http://eur-lex.europa.eu/legal-content/EN/TXT/?qid=1429879014532&uri=URISERV:l28186, accessed in October 2014.

[2] H. Engerer, M. Horn, Energ. Policy, 38 (2010) 1017-1029.

[3] Y. Traa, B. Burger, J. Weitkamp, Micropor. Mesopor. Mat., 30 (1999) 3-41.

[4] J.N. Armor, Catal. Today, 26 (1995) 147-158.

[5] Z. Sobalik, in: S.L. Suib (Ed.) New and Future Developments in Catalysis: Catalysis for Remediation and Environmental Concerns, Elsevier, 2013, pp. 155-194.

[6] Y. Nishizaka, M. Misono, Chem. Lett., (1993) 1295-1298.

[7] C.J. Loughran, D.E. Resasco, Appl. Catal., B, 7 (1995) 113-126.

[8] H. Ohtsuka, T. Tabata, Appl. Catal., B, 21 (1999) 133-139.

[9] A.P. Ferreira, C. Henriques, M.F. Ribeiro, F.R. Ribeiro, Catal. Today, 107–108 (2005) 181-191.

[10] A.P. Ferreira, S. Capela, P. Da Costa, C. Henriques, M.F. Ribeiro, F.R. Ribeiro, Catal. Today, 119 (2007) 156-165.

[11] J.A.Z. Pieterse, S. Booneveld, Appl. Catal., B, 73 (2007) 327-335.

[12] I.O. Costilla, M.D. Sanchez, M. Alicia Volpe, C.E. Gigola, Catal. Today, 172 (2011) 84-89.

[13] J.A.Z. Pieterse, R.W. van den Brink, S. Booneveld, F.A. de Bruijn, Appl. Catal., B, 46 (2003) 239-250.

[14] J.A.Z. Pieterse, R.W. van den Brink, S. Booneveld, F.A. de Bruijn, in: E. VanSteen, M. Claeys, L.H. Callanan (Eds.) Recent Advances in the Science and Technology of Zeolites and Related Materials, 2004, pp. 2522-2526.

[15] H.Y. Chen, X. Wang, W.M.H. Sachtler, Appl. Catal., A, 194 (2000) 159-168.

[16] O. Gorce, F. Baudin, C. Thomas, P. Da Costa, G. Djega-Mariadassou, Appl. Catal., B, 54 (2004) 69-84.

[17] E.M. Holmgreen, M.M. Yung, U.S. Ozkan, Appl. Catal., B, 74 (2007) 73-82.

[18] H. Decolatti, H. Solt, F. Lonyi, J. Valyon, E. Miro, L. Gutierrez, Catal. Today, 172 (2011) 124-131.

[19] S.T. Homeyer, W.M.H. Sachtler, Appl. Catal., 54 (1989) 189-202.

[20] B.J. Adelman, W.M.H. Sachtler, Appl. Catal., B, 14 (1997) 1-11.

[21] S.N. Reifsnyder, M.M. Otten, H.H. Lamb, Catal. Today, 39 (1998) 317-328.

[22] A. Trovarelli, Cat. Rev. - Sci. Eng., 38 (1996) 439-520.

[23] H.L. Tidahy, S. Siffert, J.F. Lamonier, R. Cousin, E.A. Zhilinskaya, A. Aboukais, B.L. Su, X. Canet, G. De Weireld, A. Frere, J.M. Giraudon, G. Leclercq, Appl. Catal., B, 70 (2007) 377-383.

[24] Y.-S. Bi, G.-Y. Dang, X.-H. Zhao, X.-F. Meng, H.-J. Lu, J.-T. Jin, J. Hazard. Mater., 229–230 (2012) 245-250.

[25] A.M. de Oliveira, I. Costilla, C. Gigola, I.M. Baibich, V.T. da Silva, S.B.C. Pergher, Catal. Lett., 136 (2010) 185-191.

[26] Z.J. Li, M. Flytzani-Stephanopoulos, J. Catal., 182 (1999) 313-327.

[27] A.B. Gaspar, L.C. Dieguez, Appl. Catal., A, 201 (2000) 241-251.

[28] K.I. Hadjiivanov, G.N. Vayssilov, Adv. Catal., 47 (2002) 307-511.

[29] V. Gruver, J.J. Fripiat, Journal of Physical Chemistry, 98 (1994) 8549-8554.

[30] M. Armandi, B. Bonelli, E. Garrone, M. Ardizzi, F. Cavani, L. Dal Pozzo, L. Maselli, R. Mezzogori, G. Calestani, Appl. Catal., B, 70 (2007) 585-596.

[31] A.M. Bradshaw, F.M. Hoffmann, Surf. Sci., 72 (1978) 513-535.

[32] M. Daturi, C. Binet, J.C. Lavalley, A. Galtayries, R. Sporken, Phys. Chem. Chem. Phys., 1 (1999) 5717-5724.

[33] P.S.F. Mendes, G. Lapisardi, C. Bouchy, M. Rivallan, J.M. Silva, M.F. Ribeiro, Appl. Catal., A, Article in press (2015).

[34] P. Li, Y. Xiang, V.H. Grassian, S.C. Larsen, J. Phys. Chem. B, 103 (1999) 5058-5062.

[35] P. Gelin, M. Primet, Appl. Catal., B, 39 (2002) 1-37.

[36] L. Gutierrez, E.A. Lombardo, Appl. Catal., A, 360 (2009) 107-119.

[37] L. Gutierrez, A. Boix, J.O. Petunchi, J. Catal., 179 (1998) 179-191.

[38] S. Capela, R. Catalao, M.F. Ribeiro, P. Da Costa, G. Djega-Mariadassou, F.R. Ribeiro, C. Henriques, Catal. Today, 137 (2008) 157-161.
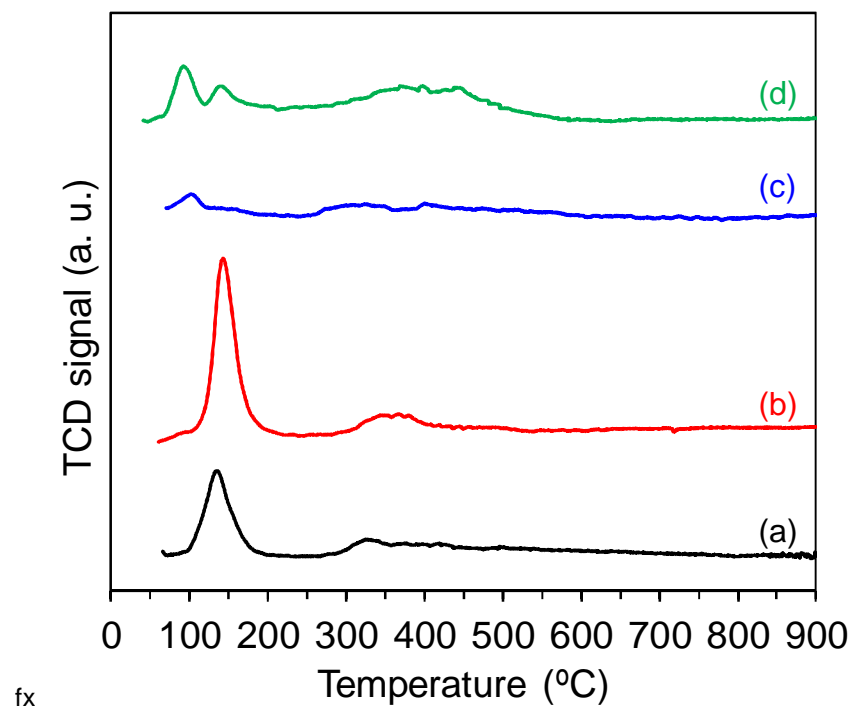
Figure 1 – H_2-TPR profiles: Pd(0.3)-HMOR (**a**), Pd(0.3)Ce(2)-HMOR (**b**), Pd(0.3)-HBEA (**c**) and Pd(0.3)Ce(2)-HBEA (**d**).
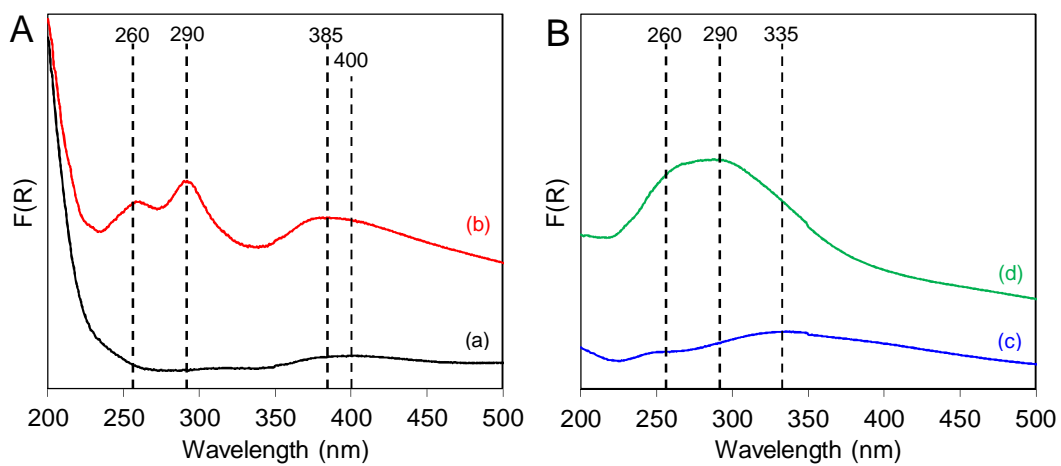
Figure 2 – DRS UV-Vis spectraof MOR (A) and BEA (B) catalysts: Pd(0.3)-HMOR (**a**), Pd(0.3)Ce(2)-HMOR (**b**), Pd(0.3)-HBEA (**c**) and Pd(0.3)Ce(2)-HBEA (**d**).
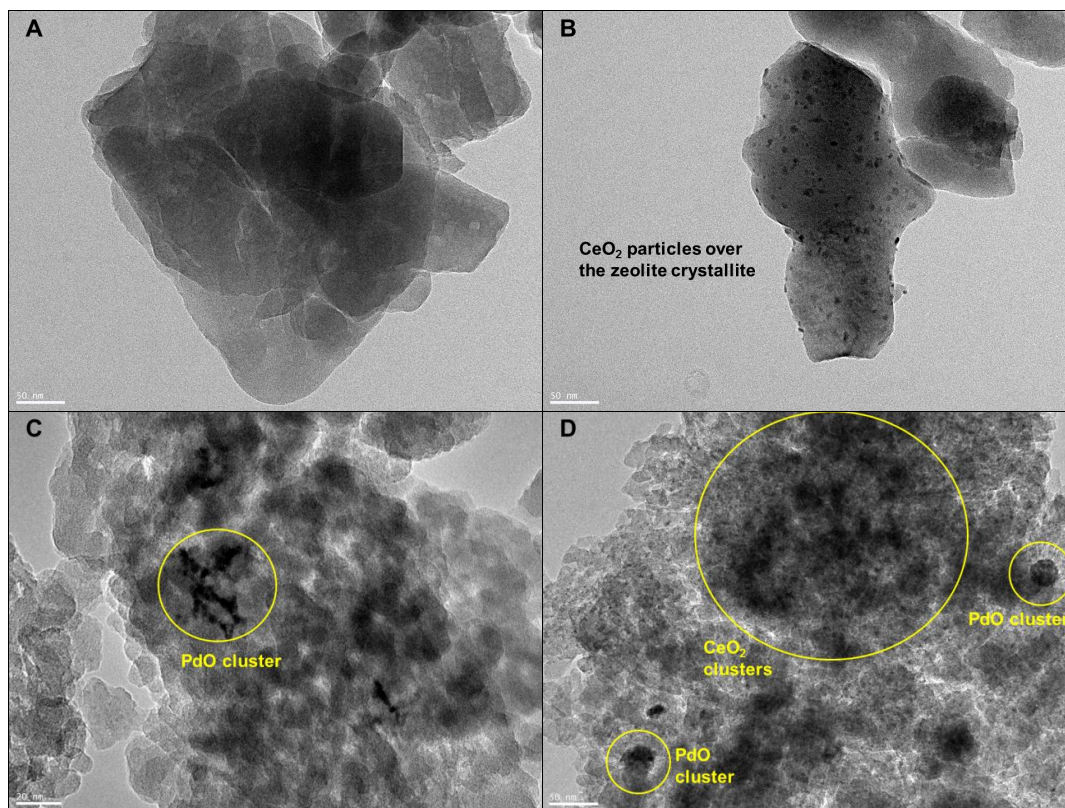
Figure 3 – TEM images: Pd(0.3)-HMOR (A), Pd(0.3)Ce(2)-HMOR (B), Pd(0.3)-HBEA (C) and
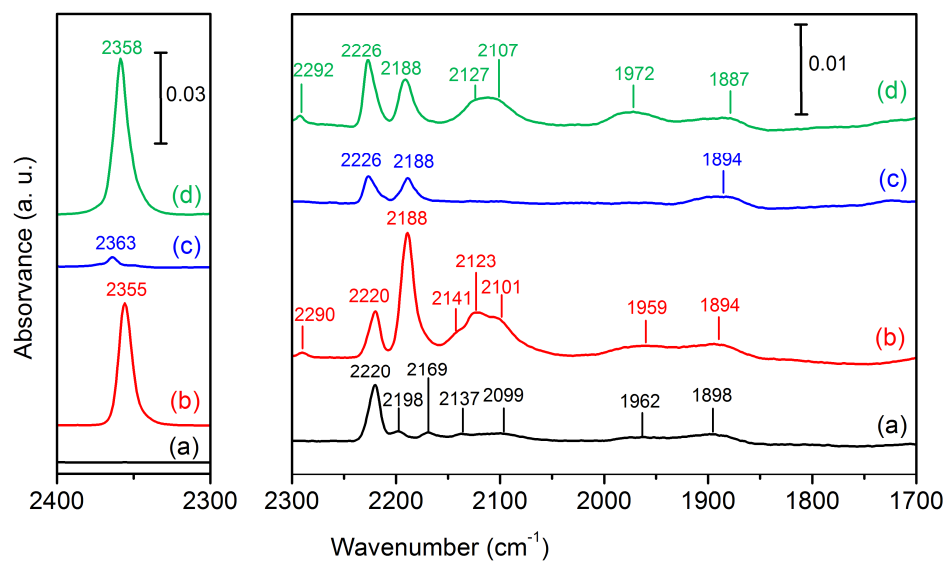
Pd(0.3)Ce(2)-HBEA (D).

Figure 4 – FTIR spectra of reduced catalysts at room temperature, after 5 torrCO exposure: Pd(0.3)-

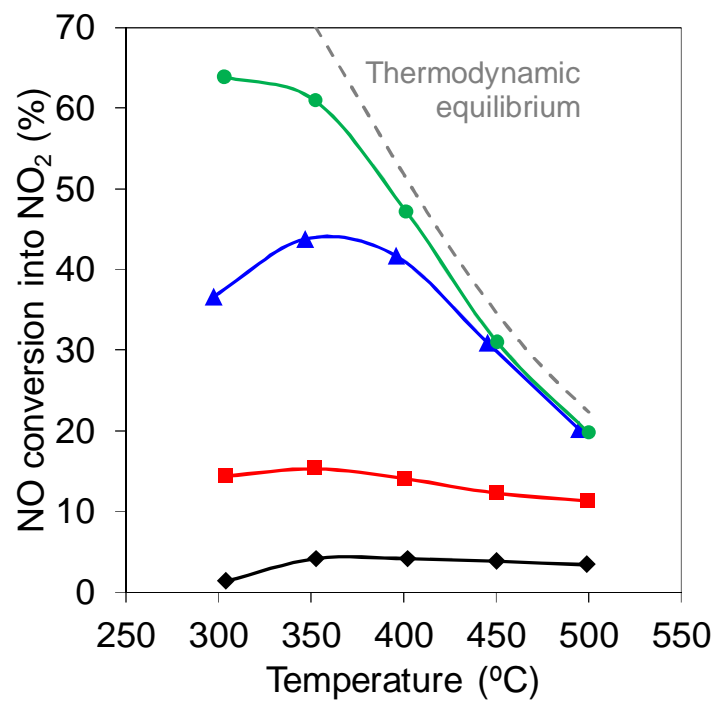HMOR (**a**), Pd(0.3)Ce(2)-HMOR (**b**), Pd(0.3)-HBEA (**c**) and Pd(0.3)Ce(2)-HBEA (**d**).

Figure 5 – NO conversion into NO_2 of Pd(0.3)-HMOR (♦), Pd(0.3)Ce(2)-HMOR (■), Pd(0.3)-HBEA (▲)

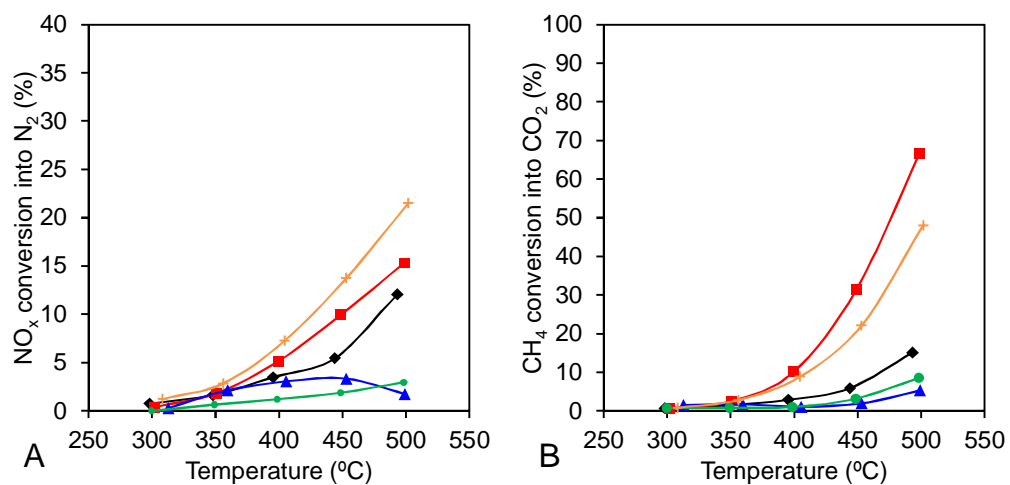and Pd(0.3)Ce(2)-HBEA (●) with 1000 ppm NO, 7% O_2 and GHSV = 40000 h^{-1}.

Figure 6 – NO conversion into N_2 (A) and CH_4 conversion into CO_2 (B) of Pd(0.3)-HMOR (♦) ,

Pd(0.3)Ce(2)-HMOR (■), Pd(0.3)-HBEA (▲), Pd(0.3)Ce(2)-HBEA (●) and dual bed (+) with 1000 ppm

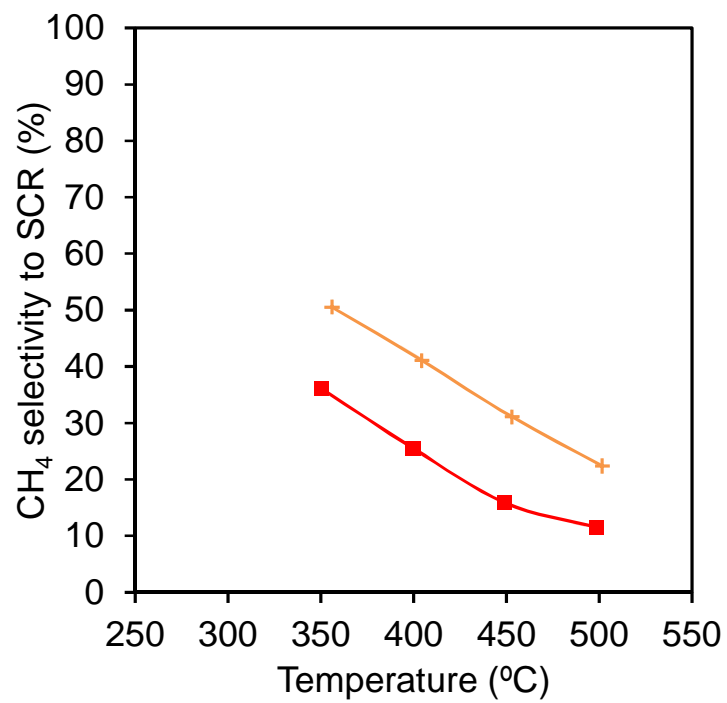NO, 1000 ppm CH_4, 7 vol.% O_2, 2 vol.% of H_2O and GHSV = 40000 h^{-1}.

Figure 7 – CH$_4$ selectivity to SCR reaction Pd(0.3)Ce(2)-HMOR (■) and dual bed (+) with 1000 ppm NO, 1000 ppm CH$_4$, 7 vol.% O$_2$, 2 vol.% of H$_2$O and GHSV = 40000 h^{-1}.
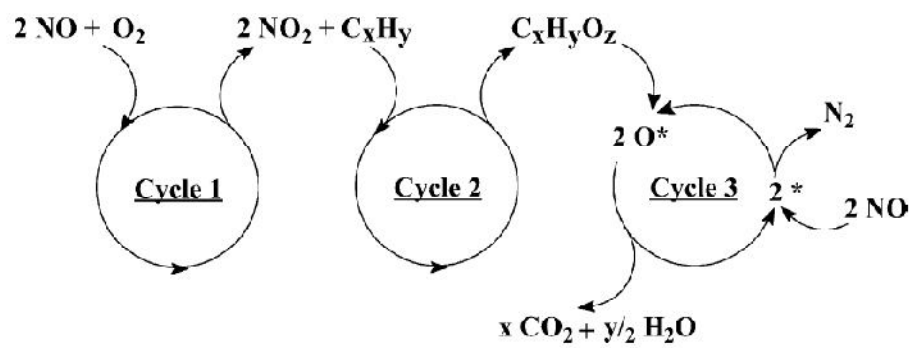
Figure 8 – 3-funtion HC-SCR mechanism (reproduced from [16]). Each cycles corresponds to a function.

List of Tables

Table 1 – Comparison of catalytic test conditions and NO_x conversion between Pd(0.3)Ce(2)-HMOR and other catalysts reported in literature.

	Similar formulations				Similar [NO]/[CH$_4$]		
Catalyst	Pd(0.4)Ce(2-4) -HMOR			Pd(0.2)Ce (2) -HMOR	Pt(0.39)Co(2. 87) -HMOR	Co(1.7)La(1 .2) -HMOR	Pd(0.3)Ce (2) -HMOR
Reference	[14]			[12]	[37]	[36]	This work
[NO] / [CH$_4$] (ppm)	500 / 2500	240 / 1750	117 / 2260	1010 / 3300	**1000 / 1000**	**1000 / 1000**	**1000 / 1000**
GHSV (h^{-1})	1700 0	1700 0	1700 0	33000	**30000**	**7500**	**40000**
T (ºC)	375	385	385	500	500	500	500
NO$_x$ conversi on	60%	80%	100 %	65%	**36%**	**40%**	**15%**